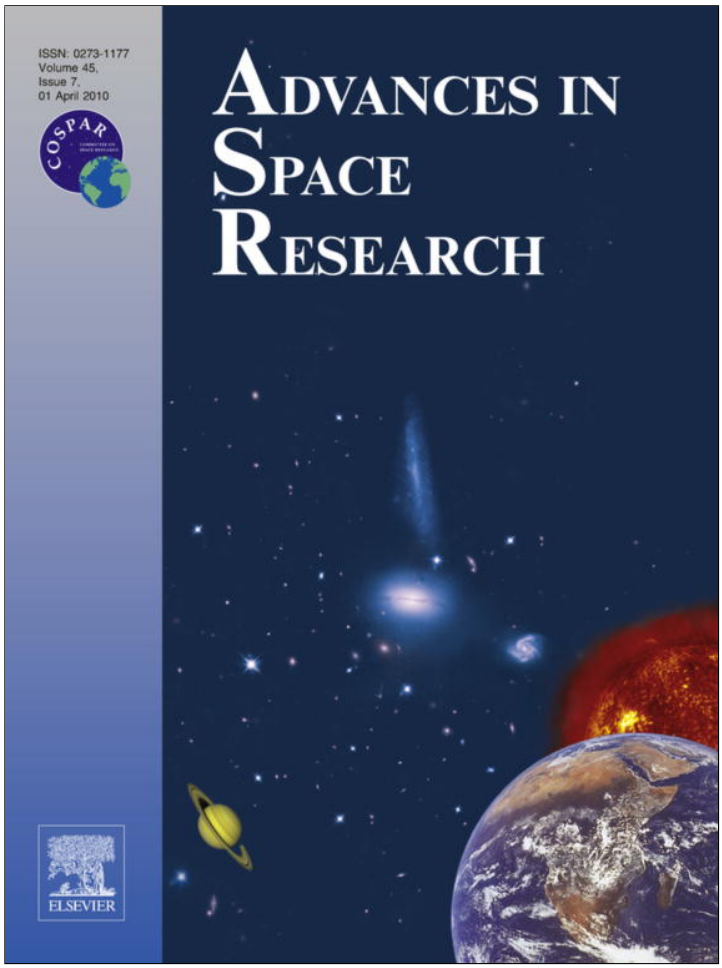

Available online at www.sciencedirect.com
ScienceDirect
Advances in Space Research 45 (2010) 850–857
ADVANCES IN SPACE RESEARCH (a COSPAR publication)
www.elsevier.com/locate/asr

Comparison of organ dose and dose equivalent for human phantoms of CAM vs. MAX

Myung-Hee Y. Kim [a,*], Garry D. Qualls [b,1], Tony C. Slaba [c,2], Francis A. Cucinotta [d,3]

[a] Universities Space Research Association, 2101 NASA Parkway, Houston, TX 77058, USA
[b] NASA Langley Research Center, Hampton, VA 23681-2199, USA
[c] Old Dominion University, E&CS Building, Elkhorn Ave., Norfolk, VA 23529, USA
[d] NASA Johnson Space Center, 2101 NASA Parkway, Houston, TX 77058, USA

Received 30 January 2009; received in revised form 15 September 2009; accepted 16 September 2009

Abstract

For the evaluation of organ dose and dose equivalent of astronauts on space shuttle and the International Space Station (ISS) missions, the CAMERA models of CAM (Computerized Anatomical Male) and CAF (Computerized Anatomical Female) of human tissue shielding have been implemented and used in radiation transport model calculations at NASA. One of new human geometry models to meet the "reference person" of International Commission on Radiological Protection (ICRP) is based on detailed Voxel (volumetric and pixel) phantom models denoted for male and female as MAX (Male Adult voXel) and FAX (Female Adult voXel), respectively. We compared the CAM model predictions of organ doses to those of MAX model, since the MAX model represents the male adult body with much higher fidelity than the CAM model currently used at NASA. Directional body-shielding mass was evaluated for over 1500 target points of MAX for specified organs considered to be sensitive to the induction of stochastic effects. Radiation exposures to solar particle event (SPE), trapped protons, and galactic cosmic ray (GCR) were assessed at the specific sites in the MAX phantom by coupling space radiation transport models with the relevant body-shielding mass. The development of multiple-point body-shielding distributions at each organ made it possible to estimate the mean and variance of organ doses at the specific organ. For the estimate of doses to the blood forming organs (BFOs), data on active marrow distributions in adult were used to weight the bone marrow sites over the human body. The discrete number of target points of MAX organs resulted in a reduced organ dose and dose equivalent compared to the results of CAM organs especially for SPE, and should be further investigated. Differences of effective doses between the two approaches were found to be small (<5%) for GCR.

Keywords: Organ dose and dose equivalent; Human tissue models; Risk assessment; Solar particle events; Galactic cosmic ray; Radiation protection

1. Introduction

Exposure to space radiation is an occupational hazard for astronauts in space missions such as the International Space Station (ISS) and future missions to Moon and Mars. Astronauts may participate in more than one ISS mission, space shuttle mission, or future lunar missions. The cumulative risk across several missions, and the lifetime risks for cancer, cataract, and other diseases from space radiation exposures are a major concern (Cucinotta and Durante, 2006; Cucinotta et al. 2001a, 2001b; NCRP, 2000; NRC, 2005; Schimmerling et al. 2003; White and Averner, 2001). The large uncertainties in the estimations of these risks have led to a rigorous radiobiological research program at NASA.

A major focus of NASA's radiation protection program is to monitor career effective doses for individual astronauts and best efforts are used to keep the risk as low as reasonably

* Corresponding author. Tel.: +1 281 244 2993; fax: +1 281 483 3058.
E-mail addresses: myung-hee.y.kim@nasa.gov (Myung-Hee Y. Kim), garry.d.qualls@nasa.gov (G.D. Qualls), tony.c.slaba@nasa.gov (T.C. Slaba), francis.a.cucinotta@nasa.gov (F.A. Cucinotta).
[1] Tel.: +1 757 864 4442.
[2] Tel.: +1 757 864 1420.
[3] Tel.: +1 281 483 0968.

0273-1177/$36.00 © 2009 COSPAR. Published by Elsevier Ltd. All rights reserved.
doi:10.1016/j.asr.2009.09.027

achievable (ALARA) (NCRP, 2002; Cucinotta et al. 2008). The equivalent dose in an organ or tissue is the product of the average absorbed dose over the tissue or organ and the defined radiation weighting factor for a given type and energy of the radiation incident and it is summed over all radiations causing the dose. The effective dose is defined as the sum of weighted equivalent doses in the specified tissues and organs of the body (ICRP, 2007) for cancer risks in radiation protection practices. Radiation exposure limits for astronauts corresponding to a 3% risk of exposure-induced death (REID) from fatal cancer calculated from the effective dose are given as career limits for missions in low Earth orbit (LEO) (NCRP, 2000, 2002) and recommended for lunar and Mars missions (NCRP, 2006).

Numerous measurements of space radiation exposures were performed with crew personal dosimeters using thermoluminescence detectors (TLDs) and nuclear track detectors (CR39) and with environmental dosimeters employing in addition instruments, such as tissue equivalent proportional counters (TEPC) and particle spectrometers. However, such measurements have not yet been used for the evaluation of crew organ dose equivalents but used for the consistency checks of the transport models. Because crew personnel dosimeters of TLDs do not account for radiation quality or organ shielding by body tissue, the radiation shielding by body tissue at specific organ sites were accounted for by using ray tracing in the human phantom models of CAM and CAF (Billings et al. 1973). Individual organ dose equivalents were determined by scaling the calculated doses to the measurements of the area together with the astronaut dosimeter results (Cucinotta et al. 2008). Organ doses were measured in some phantom experiments (Badhwar et al. 2002) and Cucinotta et al. (2008) published a comparison between measurements and calculations. NASA's space radiation transport models of organ dose equivalents, BRYNTRN (Cucinotta et al. 1994; Wilson et al. 1989) and HZETRN (Wilson et al., 1991) with QMSFRG (Cucinotta et al. 2006), were used to estimate the effective dose for astronauts upon their return from space missions.

For accurate organ dose and dose equivalent assessments, an anatomically correct geometric model of the different tissues is considered important, because the characteristic primary radiation environment at a specific organ site varies considerably in traversing tissue within the human body. The body geometry models of CAM and CAF represent the 50th percentile Air Force male and female bodies, respectively (Billings et al. 1973). In recent years, several new human phantoms have been developed for risk analysis. New models are designed to address possible shortcomings of the older models, and to reflect the analysis recommendations of national and international committees. New human geometry models denoted for male and female as MAX (Male Adult voXel) (Kramer et al. 2003) and FAX (Female Adult voXel) (Kramer et al. 2004), respectively, are based upon Computed Tomography (CT) scans of human bodies and closely resemble the "Reference Adults" of the International Commission on Radiological Protection (ICRP). A new tissue model of MAX was implemented for the evaluation of directional body-shielding mass at evenly distributed target points throughout each major organ.

Radiation doses due to solar particle event (SPE), trapped protons, and galactic cosmic ray (GCR) were assessed at numerous sites in the human body by coupling space radiation transport models with the detailed body shielding masses of the phantom models of CAM and MAX. From the multiple-point body-shielding distributions at each organ of MAX, the mean and variance of the organ dose was estimated, by which the dose–response relationship can be assessed for the acute risk. For the estimate of the blood forming organ (BFO) dose, the detailed distributions of active marrow in adults (Cristy, 1981) were implemented at bone marrow sites over the human body. We report the detailed comparison between CAM and MAX models in terms of organ dose (in Gy-Eq) and the effective dose (in Sv) obtained from the organ dose equivalents, for various radiation environments, including those at ISS orbit.

The discrete number of target points used at the MAX organ in the current study resulted in the underestimating of the organ dose and dose equivalent compared to the results of CAM. Assessments of organ averaged dose and dose equivalent of MAX were dependent on the number of target points at the organ (Slaba et al. 2009). Because the ICRP reference male values of density, mass, and volume for major organs are represented very well by MAX, the dose assessment is expected to be accurate at the specific site. However, for the convergence of organ averaged dose equivalent of MAX phantom, more target points are necessary than are currently considered points of over 1500 sites as discussed in the mass averaged error analysis by Slaba et al. (2009). In the current study, the difference between CAM and MAX for the effective dose calculations from GCR exposure was less than 5%, with little dependence on spacecraft thickness; while relatively large differences were observed for thin spacecraft thicknesses due to solar- and trapped-protons. However, for a moderately-thick spacecraft, the difference was reduced to within the error range of 10% for the exposure to those protons. The resultant effective dose from the converged organ dose equivalents of MAX phantom would narrow the difference between CAM and MAX for the cancer risk of exposure to various space radiation environments.

2. Model description for the evaluation of space radiation risk

2.1. NASA operational procedure for the space radiation at LEO

As an effective operational radiation safety program for astronauts in LEO (Cucinotta et al. 2008), the radiation cancer risk and organ doses have been assessed and recorded at NASA. Based on crew personnel dosimeters

(TLDs) of the measurements of absorbed dose at the skin in space flights, astronauts' organ dose and dose equivalent were estimated from space radiation transport models by accounting for radiation quality and organ shielding through the human geometry models of CAM and CAF (Billings et al. 1973). The effective dose, E, is defined as the sum of weighted equivalent doses, H_T, over specified tissues and organs of the body for radiation cancer risk (NCRP, 2000, 2002) using the tissue weighting factors, w_T (ICRP, 2007). The organ dose equivalent, $\overline{H}_T$, is determined as an average of H_T over all points in the organ or tissue, and NCRP adopted $\overline{H}_T$ as an acceptable approximation for H_T for space radiation (NCRP, 2002). Therefore, the organ dose equivalents with the corresponding tissue/organ weighting factors, w_T (ICRP, 2007), were used for the approximation of the effective dose for space radiation,

$$E = \sum_T w_T H_T \approx \sum_T w_T \overline{H}_T. \quad (1)$$

Procedures in NASA's operational radiation protection program to estimate the organ dose and the radiation cancer risk from the effective dose in Eq. (1) are depicted in Fig. 1, in which the radiation dose measurement at the skin ('Personal dosimeter measurement' in Fig. 1) is related to the specific organ dose. Physical dose estimates of astronauts from the space radiation exposure on various space shuttle missions and ISS space flights were made according to this procedure, and the results have been reported in detail (Cucinotta et al. 2008).

2.2. Tissue models for CAM and MAX and the recent ICRP weighting factor

The radiation environment in a spacecraft, which consists of protons, heavy ions, and secondary neutrons, is further modified at each anatomical location by passing through body tissue. The human geometry model CAM included variations of material density and fractional composition by weight due to the principal chemical elements contained in muscle, bone, bone marrow, and organ tissue. For the human geometry model MAX, the specific tissue type of each voxel (volumetric and pixel) in Computed Tomography (CT) scan was identified by Kramer et al. (2003) from the segmentation process with the associated data value of Hounsfield number, which is a normalized index of X-ray attenuation based on a scale of −1000 for air to +1000 for bone, with water being zero. The organ target point distributions used with MAX were defined by Slaba et al. (2009) using surface and interior meshes based on the implicit geometry method (Perrson, 2005). To account for the radiation transport properties within the human body, directional distributions of areal density for CAM and MAX were applied at the specified locations in the body. Table 1 shows the elemental composition of representative tissue models for CAM and MAX. For the effective dose, ICRP has revised its 1990 recommendations (ICRP, 1990). The recently recommended weighting factors (ICRP, 2007) have been implemented with the two tissue shielding assumptions for the comparison of risk assessments for the human geometry models of CAM and MAX.

2.3. Multiple target points and BFO marrow distributions for radiation risk estimation

The absorbed dose at a organ site due to energy deposition by all particles from space radiation were estimated using ray tracing for CAM and MAX, and the organ dose equivalent were obtained from the absorbed dose multiplied by the accepted quality factors Q defined by

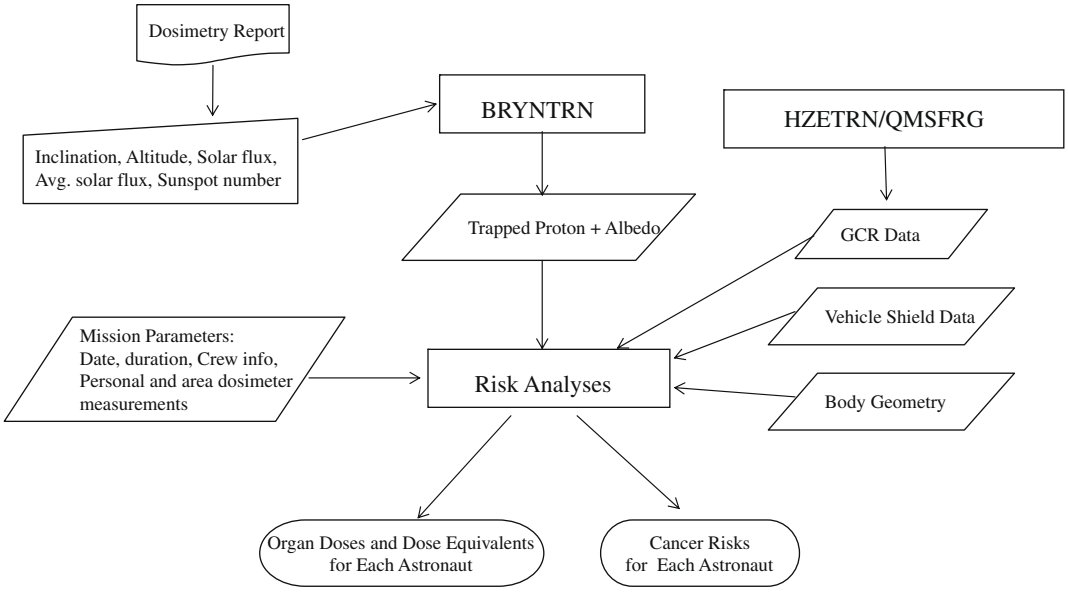

Fig. 1. NASA's operational radiation protection procedure for post-flight assessment of organ dose/dose equivalents and effective doses as used on the ISS and STS programs. A similar procedure would be used in the future for lunar and Mars missions, however modified by likely differences in dosimetry methods.

Table 1
Elemental composition and bulk density of human tissue model for CAM and MAX.

CAM		MAX		
Atom	wt%	Atom	wt%	Renormalized wt%
H	11.11	H	10	10.4
		C	23	23.8
O	88.89	N	2.6	2.7
		O	61	63.1
Sum	100	Sum	96.6	100
ρ, g/cm^3	1.0	ρ, g/cm^3	1.0	

the International Commission on Radiological Protection in 1990 (ICRP, 1990). The quality factors relate the biological damage incurred from any ionizing radiation to the damage produced by γ-rays. In general, they are a function of linear energy transfer (LET), which depends on both particle type and energy. These organ dose equivalents were used for the calculation of effective dose in Eq. (1) for cancer risk estimation. Table 2a lists various organ/tissue sites of CAM and their weighting factors (ICRP, 2007) for effective dose calculation, and Table 2b lists the number of target points currently considered at each MAX organ/tissue sites with the corresponding weighting factor. Detailed information of target points currently considered at the remainder of the MAX organ/tissue sites is also listed in Table 2c.

For the deterministic acute effects, the quality factors for the dose equivalent generally overestimates the relative biological effectiveness (RBE), and the National Council for Radiological Protection (NCRP, 2000) has recommended that risks for non-cancer or deterministic effects be made in terms of an alternate dose quantity denoted as the Gray-Equivalent (Gy-Eq) using radiation field dependent RBE for specific components, because distinct radiation quality functions occur for acute radiation risks and cancer. The Gray-Equivalent, G_T, is defined as

Table 2a
CAM organ/tissue and weighting factors defined by ICRP 103 (2007).

Organ/tissue	w_T
Avg. skin	0.01
Eye	0.00
Avg. BFO	0.12 (bone marrow) + 0.01 (bone surface)
Stomach	0.12
Colon	0.12
Liver	0.04
Lung	0.12
Esophagus	0.04
Bladder	0.04
Thyroid	0.04
Chest/breast	0.12
Gonads	0.08
Front brain	0.01
Mid brain	
Rear brain	
Salivary gland	0.01
Remainder	0.12
Sum	1.00

Table 2b
MAX organ/tissue and weighting factors defined by ICRP 103 (2007).

Organ/tissue	Number of points	w_T
BFO_mandible	10	0.12 (bone marrow) + 0.01 (bone surface)
BFO_pelvis	25	
BFO_ribs	22	
BFO_skull	26	
BFO_spine	25	
BFO_upper_left_arm	21	
BFO_upper_left_leg	22	
BFO_upper_right_arm	21	
BFO_upper_right_leg	21	
Bladder	13	0.04
Breast	10	0.12
Colon_large_intestine	13	0.12
Liver	10	0.04
Lungs	19	0.12
Esophagus	12	0.04
Skin_head_and_neck	102	0.01
Skin_left_arm	100	
Skin_lower_legs	225	
Skin_lower_torso	94	
Skin_mid_torso	90	
Skin_right_arm	94	
Skin_upper_legs	197	
Skin_upper_torso	96	
Stomach	13	0.12
Testes	10	0.08
Thyroid	8	0.04
Brain	41	0.01
Salivary glands	12	0.01
ΣRemainder	186	0.12
Lens	2	0.00
Retina	2	
Sum	1542	1.00

Table 2c
Remainder of MAX organ/tissue with weighting factor defined by ICRP 103 (2007).

Organ/tissue	Number of points	w_T
Adrenals	9	0.12
Kidneys	13	
Pancreas	9	
Small_intestine	13	
Spleen	13	
Thymus	10	
Trachea	11	
Muscle_head_and_neck	12	
Muscle_left_arm	11	
Muscle_lower_legs	22	
Muscle_lower_torso	10	
Muscle_mid_torso	11	
Muscle_right_arm	11	
Muscle_upper_legs	20	
Muscle_upper_torso	11	
ΣRemainder	186	0.12

Table 3
Particle RBE (NCRP, 2000) and the RBE for neutrons suggested by Wilson et al. (2002) for deterministic effects.

Particle type	RBE value	
	NCRP	Suggested by Wilson et al.
Less than 1 MeV neutrons	RBE (fission neutrons)	5.0
1–5 MeV neutrons	6.0	
5–50 MeV neutrons	3.5	
Above 25 MeV neutrons	RBE (not more than those of 1–25 MeV neutrons)	3.5
Protons >2 MeV	1.5	
Heavy ions (helium, carbon, neon, argon)	2.5	
Heavy ions, all others	2.5	

$$G_T = \mathrm{RBE}_j \times D_T, \tag{2}$$

where RBE_j is a recommended value for RBE for deterministic effects for a given particle type j on the site, and D_T is the mean absorbed dose in an organ or tissue. For the estimation of organ dose from space radiation, the new dosimetric quantity of G_T was implemented using the NCRP's RBE (2000) and the suggested definition of neutron RBE (Wilson et al. 2002) for a full definition of neutron RBE. Table 3 shows the RBE as given by NCRP and the suggested RBE values for neutron fields.

For the BFO dose and dose equivalent, multiple target points were considered for both CAM and MAX, because quantitative estimates of the active bone marrow in adults are quite distributed over several body regions (Cristy, 1981), which are shown in Table 4a for 82 points of CAM, and Table 4b for 193 points of MAX. Lung is one of major cancer sites with higher cancer risk from radiation ($w_T = 0.12$) and a deep-seated organ. Accurate radiation dose of lung would be important in considering the acute risk symptom of radiation-induced vomiting for astronauts from a major SPE in future exploration missions, because a physiological response induced from high-dose irradiation was observed in the mouse lung (Fedorocko et al., 2002). The lung doses and dose equivalents and their variations from 19 target points of MAX were assessed and compared to the average quantities of CAM.

Table 4a
82 BFO target points considered for CAM and the active marrow distributions in adults calculated from anatomical data by Cristy (1981).

Body region	Number of points	Marrow distribution, %
Head and neck	9	12.2
Chest (upper torso)	13	26.1
Abdomen (mid torso)	26	24.9
Pelvis (lower torso)	17	33.4
Thighs (upper legs)	5	3.4
Lower legs	6	n/a
Arms	6	n/a
Total	82	100

Table 4b
193 BFO target points considered for MAX and the active marrow distributions in adults calculated from anatomical data by Cristy (1981).

Body region	Number of points	Marrow region	Marrow distribution, %
Spine	25	All vertebrae	42.3
Ribs	22	Thorax	24
Pelvis	25	Pelvic region	20.9
Mandible	10	Skull and arms	9.4
Skull	26		
Upper left arm	21		
Upper right arm	21		
Upper left leg	22	Legs	3.4
Upper right leg	21		
Total	193		100

3. Results and discussion

Estimates of the BFO dose at each site from the 1972 SPE inside an aluminum sphere of 5 g/cm^2 thickness during interplanetary transit showed large variations in Fig. 2a for CAM, and Fig. 2b for MAX. Such estimates at the specific point sites may be useful in biophysical

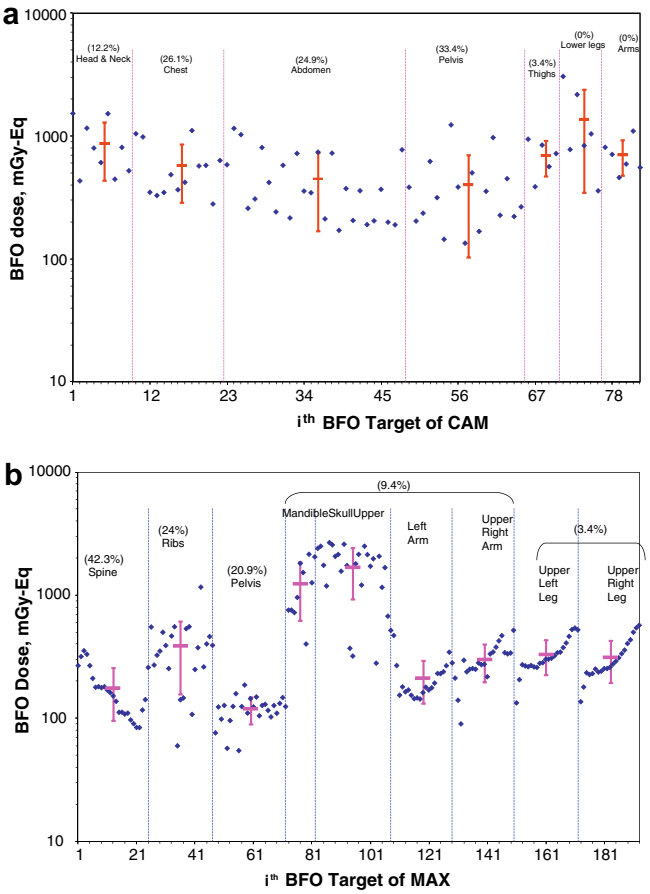

Fig. 2. Estimates of the BFO dose and the mean and variance of BFO doses in the major active marrow regions from August 1972 SPE inside an aluminum sphere of 5 g/cm^2 thickness during interplanetary transit: (a) CAM BFO targets and (b) MAX BFO targets with active marrow amounts in the parenthesis.

research to estimate the shape of the dose–response for specific diseases from the space radiation beyond LEO. In Fig. 2a and b, multiple bone marrow sites of CAM and MAX faithfully reproduced the mean and the standard deviations of the BFO dose in the major active marrow regions from the 1972 SPE. A considerable variation in BFO doses across marrow sites was found at the body regions of skull, arms, and legs, which was caused by the characteristic spectrum of proton fluence at each site. However, the active marrow at those regions contributed only a small amount. The major active marrow contribution is from the organs in deeply shielded body regions.

The calculations of the BFO dose and dose equivalent, and the BFO dose weighted by active marrow contribution are compared in Table 5a between CAM and MAX for the 1972 SPE. Because the BFO points of CAM have included variations in material density and fractional composition of principal elements by weight over the phantom, the resultant fluctuation is rather small, while that of MAX is quite large, due to the detailed type of body tissue accounted for at each point in Table 5a. To achieve the numerical convergence for a meaningful organ averaged dose and dose equivalent estimation by MAX, increased numbers of target points at each BFO site are required, as addressed by Slaba et al. (2009).

Meaningful organ average doses using a discrete number of evenly spaced target points in MAX could be made only for compact organs located in deeply shielded body regions. In contrast, it required a significantly increased number of target points for the widely-distributed organs/body regions (e.g., spine and ribs), and those organs close to the surface of body with a large solid angle exposure (e.g., brain). Therefore, the current BFO dose of MAX might be underestimated for SPE. The relatively deeply located organ lung, which is more shielded by the rest of the body tissue, showed good agreement between CAM and MAX in Table 5b. A reasonable lung dose was obtained with 19 lung points of MAX in the current calculation, and about 5–15 points had been recommended for the converged lung averaged dose by Slaba et al. (2009).

Table 5a
BFO dose and dose equivalent for CAM and MAX from the 1972 SPE.

Human geometry	No. of points	BFO dose, mGy-Eq	BFO dose weighted by active marrow amount, mGy-Eq	BFO dose eq., mSv
CAM	82	607±461	526±303	580±437
MAX	193	500±612	284±176	479±580

Table 5b
Lung dose and dose equivalent for CAM and MAX from the 1972 SPE.

Human geometry	No. of points	Lung dose, mGy-Eq	Lung dose eq., mSv
CAM	1	310	299
MAX	19	392±112	375±105

The large variation in BFO doses has opposite results when considering acute risks versus the risk of leukemia. In considering the acute risk to the BFOs, the marrow with lower dose components is fully capable of replenishing the entire blood system. Therefore, knowledge of the variation is extremely important. For leukemia risk, a linear-quadratic dose response is found with the quadratic term being dominant at high dose (>1 Gy) (NCRP, 2000). Therefore, the marrow regions with high doses are the concern since leukemia risk from a large SPE condition may contain contributions from the quadratic component of the dose–response if the dose-rate is exceeds 0.1 Gy/h.

Effective doses were estimated for CAM organs listed in Table 2a and MAX organs listed in Tables 2b and c as a function of vehicle depth. They are compared for various radiation environments in Fig. 3(a) August 1972 SPE in interplanetary space; (b) annual trapped radiation at solar minimum at ISS orbit; (c) annual GCR at solar minimum in interplanetary space; and (d) annual GCR at solar minimum at ISS orbit. In Fig. 3a and 3b, differences between the two human geometry models were relatively large for solar- and trapped-protons due to the sensitivity involved with the large number of target points of MAX for the estimate of organ averaged dose equivalents (Slaba et al. 2009). For GCR, differences converged quickly to less than 5%. This may be considered as the systematic error due to the body -shielding distribution, and to a lesser extent to the different anatomical data of marrow distributions used for CAM and MAX.

Because MAX uses all of the detailed identifications of the 3.6 mm voxels, the dose estimation at a pinpointed site of MAX can be useful knowledge to study dynamic changes in dose-rates at the specific locations in the human body. But, the current estimate of the organ dose of MAX may not be the representative quantity, because of the underestimated organ averaged dose resulting from the discrete number of target points over entire MAX organ. Many more target points should be added for each MAX organ, and the resultant estimates should be compared with spaceflight measurements for an improved risk analysis.

The variation between models will be increased further when the complexities of the spacecraft shielding distributions are included. It is necessary to consider the detailed shielding distributions of spacecraft for accurate radiation risk assessments and protection guidelines for complex radiation fields. The determinations of the mean and variance of the BFO dose equivalents in the major active marrow regions will allow more accurate estimates of the marrow response required to estimate the radiation risk of leukemia, which could be the dominant risk to astronauts from a major SPE (NCRP, 2000; BEIR, 2006).

4. Conclusion

Estimations of effective dose and radiation cancer risk at LEO have been made in the NASA operational radiation

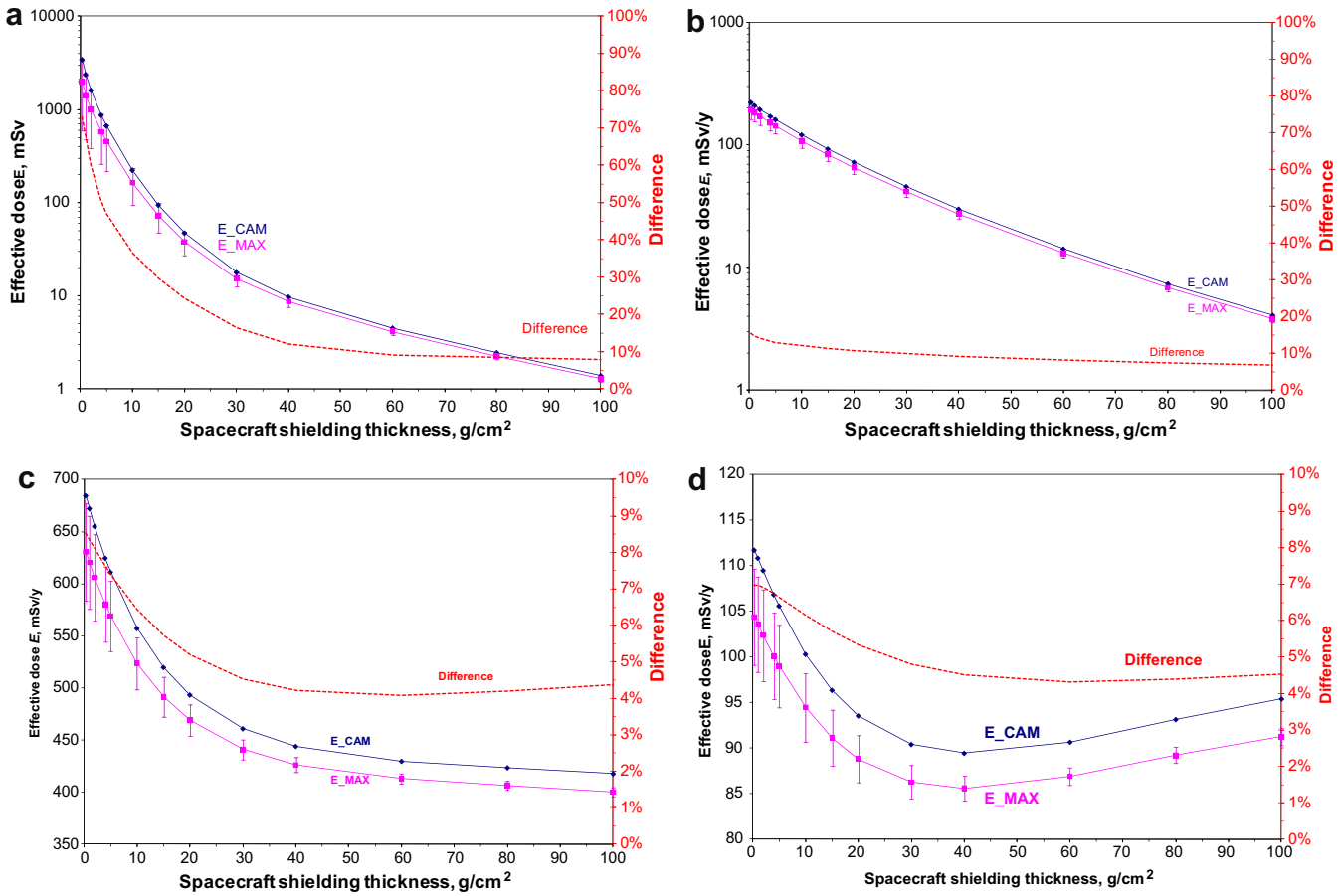

Fig. 3. Effective dose comparison between CAM and MAX and the difference between the two models (♦ for effective dose of CAM; ■ for effective dose of MAX with standard deviation; and ------ for the difference): (a) August 1972 SPE in interplanetary space; (b) annual trapped radiation at solar minimum at ISS orbit (φ = 428 MV, inclination = 51.6°, and altitude = 360 km); (c) annual GCR at solar minimum in interplanetary space; and (d) annual GCR at solar minimum at ISS orbit (φ = 428 MV, inclination = 51.6°, and altitude = 360 km).

protection program using the CAMERA models of human geometry (Cucinotta et al. 2000, 2008). In this report, we investigated more accurate representations of human organ shielding. Estimations of effective doses were made for human geometry models of CAM and MAX by implementing the tissue shielding assumptions of two models, the recently recommended weighting factors, and the detailed distribution of bone marrow sites, which were identified among many requirements for the improvement of estimation. The mean and the standard deviations of BFO dose estimates of the marrow response can be used to estimate the radiation risk of leukemia from a major SPE. The large variation in marrow doses may be important when considering acute risks to the blood system.

Because of the variations in the characteristic spectra of primary solar protons of SPEs across each target site, the detailed higher fidelity of the human geometry model of MAX itself resulted in important deviations from the CAMERA model in estimates of dose and dose equivalent at each target site for SPEs as well as more fluctuations in the organ dose and dose equivalent estimates. The mean organ doses of MAX were compared with results of CAM for the exposure to the August 1972 SPE, which is recognized as a design standard SPE for spectral variability at the median level. Consequently, organ dose differences between CAM and MAX are large for SPEs with "soft" spectra, i.e., those SPE for which the high energy portion of the spectrum falls off rapidly. For GCR and SPE with "hard" spectra, which contain a larger proportion of higher energy particles, differences are relatively small, and it would be highly unlikely these differences could be distinguished using flight dosimetry. As shielding thickness is increased, the difference between the models is reduced, especially for "soft" SPE. Shielding is considered to be the source of the systematic errors between the two geometry models requiring further investigation. For a meaningful averaged organ dose and dose equivalent estimates using MAX, many more target points were required. The effective dose estimate from over 1500 target points of the MAX major organs resulted in smaller value compared to the results from CAM for the 1972 SPE.

Many other portions of program must be improved in future work for the risk assessment and protection of astronauts. These may include new definitions of age and gender related tissue weighting factors, modified transport codes with improved neutrons production cross-sections inside

of the spacecraft, improved space environmental projection models for mission planning, and the use of detailed transport properties of structural components.

References

Badhwar, G.D., Atwell, W., Badavi, F.F., Yang, T.C., Cleghorn, T.F. Space radiation dose in a human phantom. Radiat. Res. 157, 76–91, 2002.

BEIR, BEIR Health Risks from Exposure to Low Levels of Ionizing Radiation: Biological Effects of Ionising Radiation (BEIR) VII – Phase 2, Committee to Assess Health Risks from Exposure to Low Levels of Ionizing Radiation National Research Council. National Academies Press, 2006.

Billings, M.P., Yucker, W.R., Heckman, B.R. Body Self-Shielding Data Analysis. MDC-G4131. McDonnell-Douglas Astronautics Company West, 1973.

Cristy, M. Active bone marrow distribution as a function of age in humans. Phys. Med. Biol. 26 (3), 389–400, 1981.

Cucinotta, F.A., Durante, M. Cancer risk from exposure to galactic cosmic rays: implications for space exploration by human beings. Lancet Oncol. 7, 431–435, 2006.

Cucinotta, F.A., Wilson, J.W., Badavi, F.F. Extension to the BRYNTRN code to monoenergetic light ion beams. NASA Center for AeroSpace Information, Hanover, MD, NASA TP-3472, 1994.

Cucinotta, F.A., Wilson, J.W., Williams, J.R., Dicello, J.F. Analysis of Mir-18 results for physical and biological dosimetry: radiation shielding effectiveness in LEO. Radiat. Meas. 132, 181–191, 2000.

Cucinotta, F.A., Manuel, F., Jones, J., Izsard, G., Murrey, J., Djojonegoro, B., Wear, M. Space radiation and cataracts in astronauts. Radiat. Res. 156, 460–466, 2001a.

Cucinotta, F.A., Schimmerling, W., Wilson, J.W., Peterson, L.E., Badhwar, G.D., Saganti, P., Dicello, J.F. Space radiation cancer risks and uncertainties for Mars missions. Radiat. Res. 156, 682–688, 2001b.

Cucinotta, F.A., Wilson, J.W., Saganti, P., Hu, X., Kim, M.Y., Cleghorn, T., Zeitlin, C., Tripathi, R.K. Isotopic dependence of GCR fluence behind shielding. Radiat. Meas. 41, 1235–1249, 2006.

Cucinotta, F.A., Kim, M.Y., Willingham, V., George, K.A. Physical and biological organ dosimetry analysis for International Space Station astronauts. Radiat. Res. 170, 127–138, 2008.

Federocko, P., Egyd, A., Vacek, A. Irradiation induces increased production of hematopoietic pro-inflammatory-type rcytokines in the mouse lung. Int. J. Radiat. Biol. 78, 305–313, 2002.

ICRP Publication 60 1990 Recommendations of the International Commission on Radiological Protection. Annals of the ICRP 21/1-3, 1990.

ICRP Publication 103 The 2007 Recommendations of the International Commission on Radiological Protection. Annals of the ICRP 37/2-4, 2007.

Kramer, R., Vieira, J.W., Khoury, H.J., Lima, F.R.A., Fuelle, D. All about MAX: a male adult voxel phantom for Monte Carlo calculation in radiation protection dosimetry. Phys. Med. Biol. 48, 1239–1262, 2003.

Kramer, R., Khoury, H.J., Vieira, J.W., Loureiro, E.C.M., Lima, V.J.M., Lima, F.R.A., Hoff, G. All about FAX: a female adult voxel phantom for Monte Carlo calculation in radiation protection dosimetry. Phys. Med. Biol. 49, 5203–5216, 2004.

NCRP, Radiation Protection Guidance for Activities in Low-Earth Orbit. Report No. 132, National Council on Radiation Protection and Measurements, Bethesda, MD, 2000.

NCRP, Operational Radiation Safety Program for Astronauts in Low-Earth Orbit: A Basic Framework. Report No. 142, National Council on Radiation Protection and Measurements, Bethesda, MD, 2002.

NCRP, Information Needed to Make Radiation Protection Recommendations for Space Missions Beyond Low-Earth Orbit. Report 153, Bethesda, MD, 2006.

National Research Council Committee on Review of NASA's Bioastronautics Critical Path Roadmap, Preliminary Considerations Regarding NASA's Bioastronautics Critical Path Roadmap: Interim Report, Appendix B, Bioastronautics Critical Path Roadmap (BCPR). National Academy Press, Washington, DC, 2005.

Perrson, P.-O. Mesh Generation for implicit geometries. Doctoral Dissertation, Massachusetts Institute of Technology, February 2005.

Schimmerling, W., Cucinotta, F.A., Wilson, J.W. Radiation risk and human space exploration. Adv. Space Res. 31, 27–34, 2003.

Slaba, T.C., Qualls, G.D., Clowdsley, M.S., Blattnig, S.R., Simonsen, L.C., Walker, S.A., Singleterry, R.C. Analysis of Mass Averaged Tissue Doses in CAM, CAF, MAX, and FAX, NASA Center for AeroSpace Information, Hanover, MD, NASA TP-2009-215562, April 2009.

White, R.J., Averner, M. Humans in space. Nature 409, 1115–1118, 2001.

Wilson, J.W., Townsend, L.W., Nealy, J.E., Chun, S.Y., Hong, B.S., Buck, W.W., Lamkin, S.L., Ganapole, B.D., Kahn, F, Cucinotta, F.A. BRYNTRN: a Baryon transport model. NASA Center for AeroSpace Information, Hanover, MD, NASA TP-2887, 1989.

Wilson, J.W., Townsend, L.W., Schimmerling, W., Khandelwal, G.S., Khan, F., Nealy, J.E., Cucinotta, F.A., Simonsen, L.C., Shinn, J.L., Norbury, J.W. Transport methods and interactions for space radiations. NASA Center for AeroSpace Information, Hanover, MD, NASA RP 1257; 1991.

Wilson, J.W., Kim, M.Y., De Angelis, G., Cucinotta, F.A., Yoshizawa, N., Badavi, F.F. Implementation of Gy-Eq for deterministic effects limitation in shield design. J. Radiat. Res. 43, S103–S106, 2002.